

# Temporal correlation of photons following frequency up-conversion

Lijun Ma,<sup>1</sup> Matthew T. Rakher,<sup>2</sup> Martin J. Stevens,<sup>3</sup> Oliver Slattery,<sup>1</sup>  
Kartik Srinivasan,<sup>2</sup> and Xiao Tang<sup>1,\*</sup>

<sup>1</sup>Information Technology Laboratory, National Institute of Standards and Technology, 100 Bureau Dr., Gaithersburg, MD 20899, USA

<sup>2</sup>Center for Nanoscale Science and Technology, National Institute of Standards and Technology, 100 Bureau Dr., Gaithersburg, MD 20899, USA

<sup>3</sup>Physical Measurement Laboratory, National Institute of Standards and Technology, 325 Broadway, Boulder, CO 80305, USA

\*xiao.tang@nist.gov

**Abstract:** We demonstrate an approach to measure temporal correlations of photons in the near infrared range using frequency up-conversion. In this approach, the near infrared signal photons are converted into the visible range, in which highly efficient silicon avalanche photodiodes are used to perform the temporal correlation measurements. A coherent light source and a pseudo-thermal light source were used in the experiment. The results are in agreement with theoretical values and those obtained from measurements directly made using superconducting nanowire single photon detectors. We conclude that the temporal correlation (up to 4th order) of photons was preserved in the frequency up-conversion process. We further theoretically and experimentally studied the influence of the dark counts on the measurement. The setup uses commercially available components and achieves high total detection efficiency (~26%).

©2011 Optical Society of America

**OCIS codes:** (270.5290) Photon statistics; (190.4410) Nonlinear optics, parametric processes; (230.7370) Waveguides; (030.5260) Photon counting.

---

## References and links

1. R. Hanbury Brown and R. Q. Twiss, "Correlation between photons in two coherent beams of light," *Nature* **177**(4497), 27–29 (1956).
2. M. Fox, *Quantum Optics, An Introduction* (Oxford University Press, 2006).
3. Y. Zhou, J. Liu, and Y. Shih, "Third order temporal correlation function of pseudo-thermal light," arXiv: 0909.3512v1 [quant-ph] (2009).
4. R. E. Meyers and K. S. Deacon, "Quantum ghost imaging experiments," *Proc. SPIE* **7465**, 746508 (2009).
5. H. Qian and E. L. Elson, "Fluorescence correlation spectroscopy with high-order and dual-color correlation to probe nonequilibrium steady states," *Proc. Natl. Acad. Sci. U.S.A.* **101**(9), 2828–2833 (2004).
6. P. A. Lemieux and D. J. Durian, "Investigating non-Gaussian scattering processes by using  $n$ th-order intensity correlation functions," *J. Opt. Soc. Am. A* **16**(7), 1651–1664 (1999).
7. E. A. Burt, R. W. Ghrist, C. J. Myatt, M. J. Holland, E. A. Cornell, and C. E. Wieman, "Coherence, correlations, and collisions: what one learns about Bose-Einstein condensates from their decay," *Phys. Rev. Lett.* **79**(3), 337–340 (1997).
8. H. Deng, G. Weihs, C. Santori, J. Bloch, and Y. Yamamoto, "Condensation of semiconductor microcavity exciton polaritons," *Science* **298**(5591), 199–202 (2002).
9. J. Wiersig, C. Gies, F. Jahnke, M. Aßmann, T. Berstermann, M. Bayer, C. Kistner, S. Reitzenstein, C. Schneider, S. Höfling, A. Forchel, C. Kruse, J. Kalden, and D. Hommel, "Direct observation of correlations between individual photon emission events of a microcavity laser," *Nature* **460**(7252), 245–249 (2009).
10. M. Assmann, F. Veit, M. Bayer, M. van der Poel, and J. M. Hvam, "Higher-order photon bunching in a semiconductor microcavity," *Science* **325**(5938), 297–300 (2009).
11. A. G. Palmer 3rd and N. L. Thompson, "Molecular aggregation characterized by high order autocorrelation in fluorescence correlation spectroscopy," *Biophys. J.* **52**(2), 257–270 (1987).
12. R. Hadfield, "Single-photon detectors for optical quantum information applications," *Nat. Photonics* **3**(12), 696–705 (2009).
13. M. J. Stevens, B. Baek, E. A. Dauler, A. J. Kerman, R. J. Molnar, S. A. Hamilton, K. K. Berggren, R. P. Mirin, and S. W. Nam, "High-order temporal coherences of chaotic and laser light," *Opt. Express* **18**(2), 1430–1437 (2010).

14. K. M. Rosfjord, J. K. W. Yang, E. A. Dauler, A. J. Kerman, V. Anant, B. M. Voronov, G. N. Gol'tsman, and K. Berggren, "Nanowire single-photon detector with an integrated optical cavity and anti-reflection coating," *Opt. Express* **14**(2), 527–534 (2006).
15. A. P. Vandevender and P. G. Kwiat, "High efficiency single photon detection via frequency up-conversion," *J. Mod. Opt.* **51**, 1433–1445 (2004).
16. M. A. Albota and F. N. Wong, "Efficient single-photon counting at 1.55  $\mu\text{m}$  by means of frequency upconversion," *Opt. Lett.* **29**(13), 1449–1451 (2004).
17. C. Langrock, E. Diamanti, R. V. Roussev, Y. Yamamoto, M. M. Fejer, and H. Takesue, "Highly efficient single-photon detection at communication wavelengths by use of upconversion in reverse-proton-exchanged periodically poled LiNbO<sub>3</sub> waveguides," *Opt. Lett.* **30**(13), 1725–1727 (2005).
18. E. Diamanti, H. Takesue, T. Honjo, K. Inoue, and Y. Yamamoto, "Performance of various quantum-key-distribution systems using 1.55- $\mu\text{m}$  up-conversion single-photon detectors," *Phys. Rev. A* **72**(5), 052311 (2005).
19. R. T. Thew, S. Tanzilli, L. Krainer, S. C. Zeller, A. Rochas, I. Rech, S. Cova, H. Zbinden, and N. Gisin, "Low jitter up-conversion detectors for telecom wavelength GHz QKD," *N. J. Phys.* **8**(3), 32 (2006).
20. H. Xu, L. Ma, A. Mink, B. Hershman, and X. Tang, "1310-nm quantum key distribution system with up-conversion pump wavelength at 1550 nm," *Opt. Express* **15**(12), 7247–7260 (2007).
21. H. Dong, H. Pan, Y. Li, E. Wu, and H. Zeng, "Efficient single-photon frequency upconversion at 1.06  $\mu\text{m}$  with ultralow background counts," *Appl. Phys. Lett.* **93**(7), 071101 (2008).
22. Q. Zhang, C. Langrock, M. M. Fejer, and Y. Yamamoto, "Waveguide-based single-pixel up-conversion infrared spectrometer," *Opt. Express* **16**(24), 19557–19561 (2008).
23. L. Ma, O. Slattery, and X. Tang, "Experimental study of high sensitivity infrared spectrometer with waveguide-based up-conversion detector(1)," *Opt. Express* **17**(16), 14395–14404 (2009).
24. P. Kumar, "Quantum frequency conversion," *Opt. Lett.* **15**(24), 1476–1478 (1990).
25. J. Huang and P. Kumar, "Observation of quantum frequency conversion," *Phys. Rev. Lett.* **68**(14), 2153–2156 (1992).
26. M. Rakher, L. Ma, O. Slattery, X. Tang, and K. Srinivasan, "Quantum transduction of telecommunications-band single photons from a quantum dot by frequency upconversion," *Nat. Photonics* **4**(11), 786–791 (2010).
27. L. Mandel and E. Wolf, *Optical Coherence and Quantum Optics* (Cambridge University Press, 1995).
28. M. Fejer, G. Magel, D. Jundt, and R. Byer, "Quasi-phase-matched second harmonic generation: tuning and tolerances," *IEEE J. Quantum Electron.* **28**(11), 2631–2654 (1992).
29. Datasheet of Perkin Elmer Single Photon Counting Module SPCM-AQR Series.
30. J. S. Pelc, C. Langrock, Q. Zhang, and M. M. Fejer, "Influence of domain disorder on parametric noise in quasi-phase-matched quantum frequency converters," *Opt. Lett.* **35**(16), 2804–2806 (2010).
31. M. G. Raymer, I. A. Walmsley, J. Mostowski, and B. Sobolewska, "Quantum theory of spatial and temporal coherence properties of stimulated Raman scattering," *Phys. Rev. A* **32**(1), 332–344 (1985).
32. P. Voss, Y. Su, P. Kumar, and M. Vasilyev, "Photon statistics of a single mode of spontaneous Raman scattering in a distributed Raman amplifier," *Optical Fiber Communication Conference (IEEE, 2001)*, paper WDD23.
33. Q. Lin, F. Yaman, and G. P. Agrawal, "Photon-pair generation in optical fibers through four-wave mixing: Role of Raman scattering and pump polarization," *Phys. Rev. A* **75**(2), 023803 (2007).
34. R. H. Hadfield, M. J. Stevens, R. P. Mirin, and S. W. Nam, "Single-photon source characterization with twin infrared-sensitive superconducting single-photon detectors," *J. Appl. Phys.* **101**(10), 103104 (2007).

## 1. Introduction

Temporal correlation measurements of photons are now widely used to study a variety of photon sources and their physical characteristics. In 1956, Hanbury-Brown and Twiss (HBT) first measured the photon bunching effect of thermal light in the second-order temporal correlation,  $g^{(2)}(\tau)$  [1]. Since then, second-order temporal correlation measurements using an HBT interferometer have been extensively adopted to study photon statistics of a variety of light sources [2]. Recently, higher order, e.g. third- and fourth-order ( $g^{(3)}(\tau_1, \tau_2)$  and  $g^{(4)}(\tau_1, \tau_2, \tau_3)$ ) temporal correlations have drawn more attention, since they can reveal more information about the temporal behavior of light sources and interaction media. High-order measurements are potentially useful in many research areas, including quantum imaging [3,4], light scattering [5,6], atomic and polaritonic condensates [7,8], microcavity lasers [9,10] and molecular aggregates [11]. The second-, third-, and fourth-order temporal correlations can be defined in terms of the creation ( $\hat{a}^\dagger$ ) and annihilation ( $\hat{a}$ ) operators as [2]:

$$g^{(2)}(\tau) = \frac{\langle \hat{a}^\dagger(t) \hat{a}^\dagger(t+\tau) \hat{a}(t+\tau) \hat{a}(t) \rangle}{\langle \hat{a}^\dagger(t) \hat{a}(t) \rangle^2}, \quad (1)$$

$$g^{(3)}(\tau_1, \tau_2) = \frac{\langle \hat{a}^\dagger(t) \hat{a}^\dagger(t + \tau_1) \hat{a}^\dagger(t + \tau_2) \hat{a}(t + \tau_2) \hat{a}(t + \tau_1) \hat{a}(t) \rangle}{\langle \hat{a}^\dagger(t) \hat{a}(t) \rangle^3}, \quad (2)$$

$$g^{(4)}(\tau_1, \tau_2, \tau_3) = \frac{\langle \hat{a}^\dagger(t) \hat{a}^\dagger(t + \tau_1) \hat{a}^\dagger(t + \tau_2) \hat{a}^\dagger(t + \tau_3) \hat{a}(t + \tau_3) \hat{a}(t + \tau_2) \hat{a}(t + \tau_1) \hat{a}(t) \rangle}{\langle \hat{a}^\dagger(t) \hat{a}(t) \rangle^4}, \quad (3)$$

where  $\langle \rangle$  indicates an average over time  $t$  and the  $\tau_i$ 's are time delays.

High-order temporal correlation measurements need complex and high performance experimental configurations, especially in the near infrared (NIR) range (wavelengths between 1000 nm and 2000 nm) where there is a lack of commercially available high performance single photon detectors [12]. Therefore, high-order correlation measurements are usually implemented in the visible or near visible range by using silicon-based single photon detectors [3,4]. Because the two major telecommunication wavelengths (1310 and 1550 nm) are in the NIR range, high order correlation measurements at this wavelength range are important. Recently, high order temporal correlation measurements for the NIR range were implemented by using four-element superconducting nanowire single-photon detectors (SNSPDs) [13]. However, the four-element SNSPDs used in that particular measurement had a very low detection efficiency of ~1% each. Despite recent improvements that have increased detection efficiencies above 50% [14], SNSPDs still need to work at liquid helium temperatures and are not yet widely available commercially.

Frequency up-conversion single photon detectors have recently been specifically developed for photon detection [15–21] and spectral measurement [22,23] in the NIR range. They use a nonlinear optical crystal, such as periodically poled lithium niobate (PPLN), to convert a photon in the NIR range to the visible or near visible range. The visible or near visible photons can then be detected using highly efficient, low noise and low cost silicon avalanche photodiodes (APDs).

To take advantage of the detection benefits of frequency up-conversion to the near-visible, we must confirm that the photon statistics of the source are preserved during the conversion process. A theoretical analysis of the frequency up-conversion process predicts that the quantum state should be preserved [24] and a following experiment demonstrated that nonclassical intensity correlation of twin beams is preserved after frequency conversion [25]. We recently observed that sub-Poissonian photon statistics are preserved after up-conversion [26], but a direct comparison of the statistics to theory could not be performed due to the non-idealities of the single photon source used in that work. In this work, by using up-conversion, we convert photons in the NIR region into the visible region, and then measure the temporal correlation (up to the fourth order) of the up-converted photons using Si-APDs that have high detection efficiency in this range. A coherent light source and a pseudo-thermal light source are used here, allowing for direct comparison to theory [13,27]. The goal of this experiment is to demonstrate that the temporal correlations of the up-converted photons are identical to those of the original photons, *i.e.*, the original photon statistical characteristics are preserved in the up-conversion process. If the photon statistics are preserved through up-conversion, then one can use this approach to study the statistics of the original NIR photons. We also further theoretically and experimentally study the influence of the dark counts on the temporal correlation measurements. The setup uses commercially available components and the total detection efficiency is about 26%.

## 2. Experimental configuration

The experimental configuration for measuring temporal correlations of photons in the NIR range using frequency up-conversion is shown in Fig. 1. Frequency up-conversion is based on a nonlinear optical process, known as sum frequency generation (SFG), that occurs in a 5 cm-long PPLN waveguide [28]. The signal photons near 1310 nm are converted in the waveguide to 710 nm using a pump beam. The pump beam is provided by a continuous-wave (CW)

tunable seed laser around 1550 nm followed by an erbium-doped fiber amplifier (EDFA, IPG: EAR-0.5K-C). The tunable pump laser allows the measurement to be performed for a wider signal wavelength range. Two 1310 nm/1550 nm wavelength division multiplexer (WDM) couplers are used as filters to suppress light around 1310 nm in the pump at the output of the EDFA. The amplified pump is then combined with a single photon power level signal near 1310 nm in another WDM coupler. The combined signal and pump are then coupled into the PPLN waveguide. The output light of the PPLN waveguide, including the sum frequency generated photons at 710 nm, the excess pump at 1550 nm and its second harmonic generation at 775 nm, are separated by two dispersive prisms, and only photons at 710 nm are detected for temporal correlation measurements. Band-pass interference filters are used before the Si-APDs to block other noise. The PPLN waveguide used in this experiment is 5 cm, and its quasi-phase-matching bandwidth is about 0.25 nm for 1310 nm [23]. The EDFA output power is set to 250 mW resulting in approximately 100 mW of pump light arriving at the front of PPLN waveguide following a variety of losses between EDFA and PPLN waveguide. The highest conversion efficiency is achieved when this pump power enters the waveguide. When Si-APDs (PerkinElmer SPCM-AQR-14) are used to detect the up-converted photon, the total detection efficiency is 26%, which is determined by the internal conversion efficiency inside the PPLN waveguide (80%); the transmission loss (45%); and the detection efficiency of Si-APD at the up-converted wavelength (70%). This total detection efficiency is much higher than the SNSPDs used in [13] (~1%) and also is similar to the commercially available InGaAs APDs [12] in the NIR range. Furthermore, higher quality PPLN waveguides can implement nearly 100% internal conversion efficiency [17] and the transmission loss can be further reduced by improving the coupling loss between the fiber and waveguide. Higher total detection efficiency can be realized by these improvements in an up-conversion configuration [17].

The influence of dark counts in single photon detectors is an important factor in measurements. Dark counts are defined as the counts when no signal photons are present. For an up-conversion single photon detector, the dark count rate is measured when pump light is present but the signal beam is blocked. The dark counts in this up-conversion experimental set-up originate from both the intrinsic dark counts of the Si-APD and from the counts caused by noise photons from the frequency conversion process inside the crystal. The intrinsic dark count rate of each Si-APD is very low (<100 counts/s in our experiments [29]), and is negligible in comparison to the counts caused by the noise photons due to the frequency conversion process. It is widely believed that the noise photons that arise in the frequency conversion process from the spontaneous Raman scattering (SRS) [15–20] and spontaneous parametric down conversion (SPDC) [30] generated in the waveguide by the strong pump. If these SRS photons or SPDC photons are generated at wavelengths within the signal band they can be up-converted to the detection wavelength, generating the dark counts. Because the wavelength of SPDC photons is longer than that of pump, there is no SPDC noise contribution when the pump wavelengths is longer than the signal wavelength, as in this experiment. In this case, the noise photons only occur from the anti-Stokes photons of SRS. The dark count rate in our set-up is measured to be approximately 3200 counts/s. The dark count rate is much less than that of InGaAs APDs ( $\sim 10^5$  Hz) [12], but it is significantly higher than that of SNSPDs ( $\sim 100$  Hz) [13]. Therefore, the dark count rate has to be considered when weak signals are measured.

In the experiment, two types of photon sources are used, a coherent source and a pseudo-thermal source. The coherent source is a 1310 nm CW laser, operating well above threshold and attenuated to around  $-95$  dBm using a variable optical attenuator (VOA). The pseudo-thermal source is similar to [13], in which we use a rotating ground glass disk to scatter the 1310 nm CW laser light and then use a single mode fiber (SMF-28) to collect the scattered photons in the far field. To avoid significant influence of dark counts, the detected signal photon rate is set at  $8 \times 10^5$  counts/s for both the coherent light and the pseudo-thermal light, which is two orders of magnitude larger than the dark count level.

Three half-wave plates (HWP) and polarizing beam-splitters (PBS) for 710 nm are used to split the up-converted photons, as shown in Fig. 1. Because the up-converted photons have a fixed polarization direction, the HWP and PBS combination can implement a desired split ratio, which functions as a beam splitter with tunable splitting ratio. By adjusting the HWPs, one can equally split the photons into 2, 3 or 4 beams and easily implement the second, third and fourth order temporal correlation measurements. Although second and third order temporal correlations can be obtained from a 4-split set-up, a 2 or 3 equally split set-up can do the more straightforward  $g^{(2)}(\tau)$  and  $g^{(3)}(\tau_1, \tau_2)$  measurements by 2 or 3 detectors with the same detection efficiency. In addition, the main dark counts come from the noise photons from frequency up-conversion process before the splitting and the noise photons are likewise split at the same ratio as the signal up-converted photons, therefore the ratio of signal photons to noise photons are similar for all the higher orders of temporal correlation measurement.

After splitting, the photons are detected by four Si-APDs. A four-channel time-correlated single photon counting system (PicoQuant Hydroharp 400) records photon arrival times at each detector. These time-tag data are post-processed to compute multi-start and multi-stop correlation histograms between the two, three and four channels, to obtain the  $g^{(2)}(\tau)$ ,  $g^{(3)}(\tau_1, \tau_2)$  and  $g^{(4)}(\tau_1, \tau_2, \tau_3)$ , in the same way as in [13].

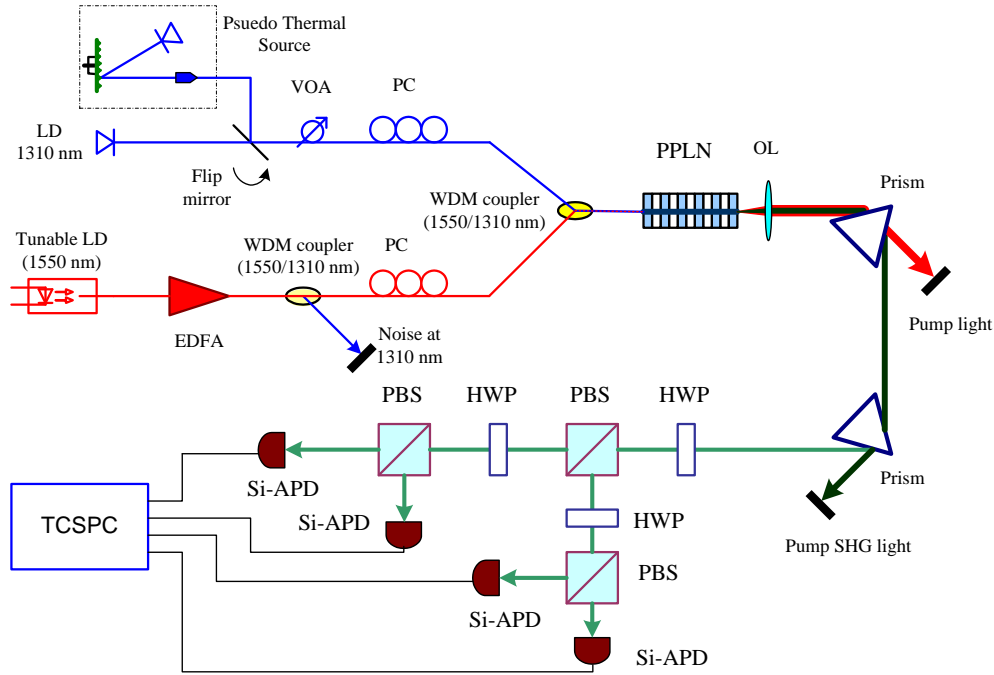


Fig. 1. Experimental configuration. LD: Laser diode, EDFA: Erbium-doped fiber amplifier; WDM: Wavelength-division multiplexing coupler; PC: Polarization controller; PPLN: Periodically poled LiNbO<sub>3</sub> waveguides; OL, Objective Lens; HWP: Half-wave plate; PBS: Polarizing beam-splitter; TCSPC: time-correlated single photon counting system.

### 3. Experimental results

The measured second-, third-, and fourth-order temporal correlation values are shown in Figs. 2, 3, and 4 (see [Media 1](#)), respectively. For coherent light, the measured data of  $g^{(2)}(\tau)$ ,  $g^{(3)}(\tau_1, \tau_2)$  and  $g^{(4)}(\tau_1, \tau_2, \tau_3)$  are close to the expected theoretical value of 1. For the pseudo-thermal source, the data shows that photons are bunched around the origin, with peak values

of  $g^{(2)}(0) = 2.001 \pm 0.035$ ,  $g^{(3)}(0,0) = 5.87 \pm 0.23$  and  $g^{(4)}(0,0,0) = 23.1 \pm 1.9$ . The peak values are in good agreement with the theoretical value of  $2! = 2$ ,  $3! = 6$  and  $4! = 24$ .

In the above experiments, the coherent source and pseudo-thermal source are near 1310 nm, while all results for  $g^{(2)}(\tau)$ ,  $g^{(3)}(\tau_1, \tau_2)$  and  $g^{(4)}(\tau_1, \tau_2, \tau_3)$  are actually measured from the up-converted photons at 710 nm. The temporal correlation results of up-converted photons are in good agreement with the theoretical results [13]. We therefore conclude that the photon statistics are well preserved in the up-conversion process. And therefore, frequency up-conversion is proved to be an accurate and highly efficient measurement method for temporal correlation of photons in the NIR region, and all components for this approach are currently commercially available.

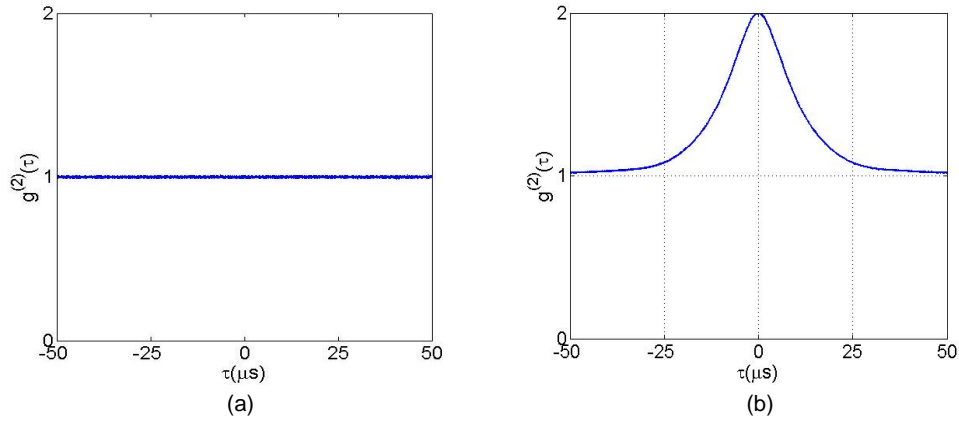


Fig. 2.  $g^{(2)}$  measurement results of (a) coherent light source and (b) pseudo-thermal source.

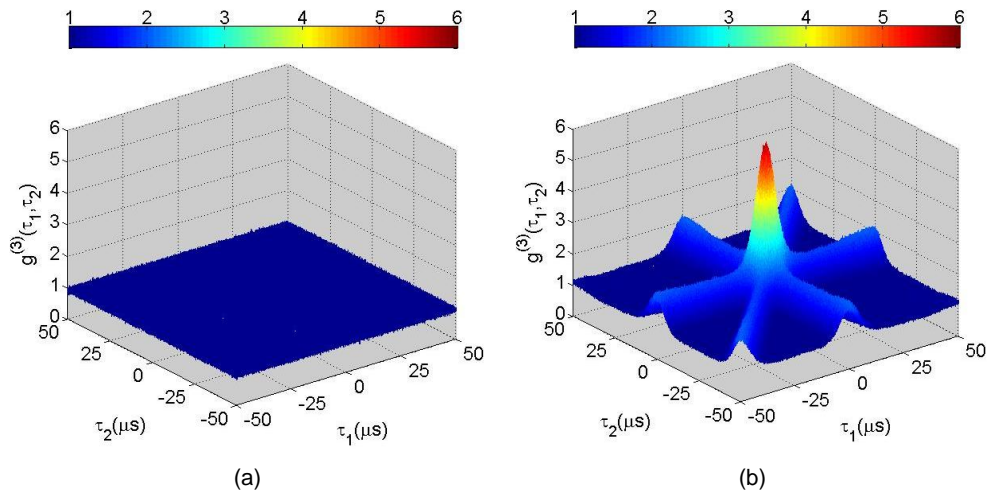


Fig. 3.  $g^{(3)}$  measurement results of (a) coherent light source and (b) pseudo-thermal source.

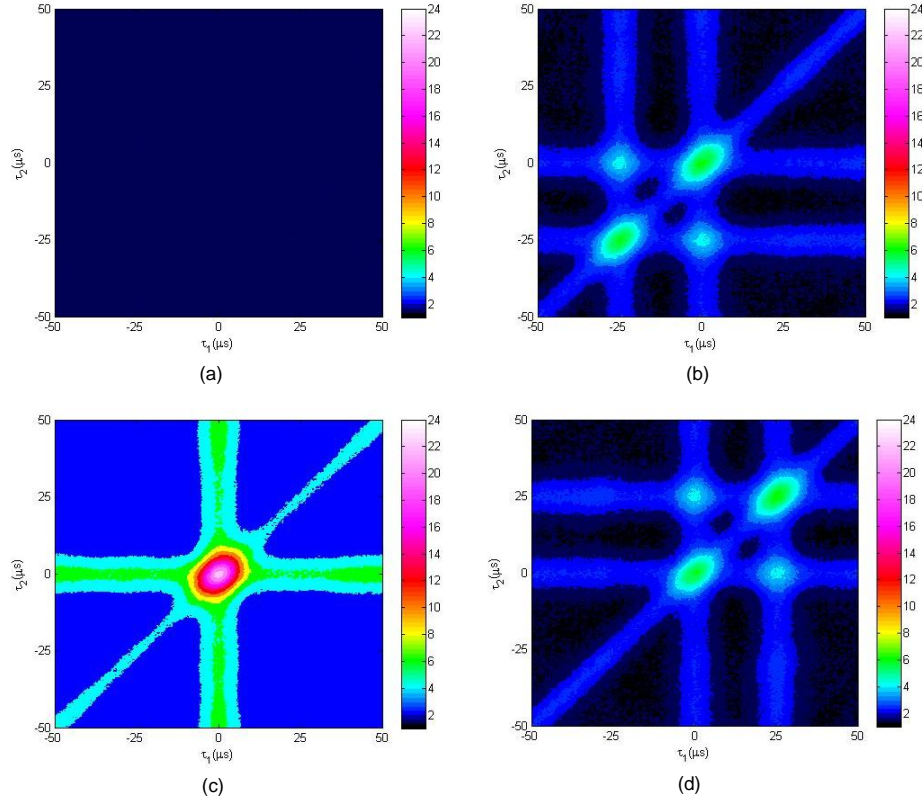


Fig. 4. Fourth-order temporal measurement results. (a) Coherent light  $g^{(4)}$  data, at  $\tau_3 = 0 \mu\text{s}$ , (b)–(d): Pseudo-thermal source  $g^{(4)}$  data at  $\tau_3 = -25 \mu\text{s}$  (b),  $\tau_3 = 0 \mu\text{s}$  (c), and  $\tau_3 = 25 \mu\text{s}$  (d). (b)–(d) are three frames of a movie showing  $g^{(4)}(\tau_1, \tau_2, \tau_3)$  (see Media 1).

#### 4. Discussion on the dark counts and their influence

Dark counts are an important factor for these temporal correlation measurements. When the signal count rate is comparable to the dark count rate, the measurement results will be significantly affected. Therefore, the influence of dark counts should be considered when the signal is weak.

To study the influence of dark counts, the dark count rate and the dark count temporal distribution should be measured. The dark count rate can be easily measured by blocking the input signal photons. We perform the temporal correlation measurements of the dark counts at different orders (2nd to 4th), and observe  $g^{(n)} \approx 1$ , without any bunching at the origin; thus, the dark count statistics, at least approximately, follow a Poissonian distribution.

As discussed in section 2, the dark counts of this frequency up-conversion set-up are mainly caused by the noise photons during this frequency conversion process. These noise photons are widely believed to be caused by the SRS of the strong pump [15–20]. Technically, these noise photons caused by SRS should follow the thermal distribution, or the Bose-Einstein distribution (BED) [31–33]. However, because of their broad spectrum, we expect the coherence time of these SRS photons to be much shorter than the temporal resolution determined by our detectors (Si-APDs) in the experiments. As a result, we are not able to observe any bunching in the temporal correlation of dark counts. Therefore, the dark counts appear to follow a Poissonian distribution for the time scale in this experiment, and we

can treat the dark counts as following a Poissonian distribution in the following analysis on the influence of dark counts.

We further take a pseudo-thermal source and vary the signal count rate to dark count rate ratio (SDR) to study the influence of the dark counts. The counts triggered by photons from a thermal source follow the BED [2]:

$$F_{thermal}(n, \mu_{sc}) = \frac{1}{\mu_{signal} + 1} \left( \frac{\mu_{signal}}{\mu_{signal} + 1} \right)^n, \quad (4)$$

where  $F_{thermal}(n, \mu_{signal})$  is the probability of  $n$  signal counts in one time slot, given the BED with mean count number  $\mu_{signal}$  in the same time slot. From the above discussion, we can treat the dark counts in this experiment as a Poissonian distribution, which is described as follows [2]:

$$F_{poiss}(n, \mu_{dark}) = \frac{\mu_{dark}^n}{n!} e^{-\mu_{dark}}, \quad (5)$$

where  $F_{poiss}(n, \mu_{dark})$  is the probability of  $n$  dark counts in a time slot, given the Poissonian distribution with mean count number  $\mu_{dark}$  in the same time slot. For a mixed signal with thermal and noise photons, the probability density function for  $n$  photons is the summation of all probabilities that the number of total photons generated from the both sources equal to  $n$ . The mixed signal probability density function can be expressed as:

$$F_{mix}(n, \mu_{signal}, \mu_{dark}) = \sum_{k=0}^n F_{thermal}(k, \mu_{signal}) \times F_{poiss}(n-k, \mu_{dark}), \quad (6)$$

where  $F_{mix}(n, \mu_{signal}, \mu_{dark})$  is the  $n$ -count probability in one time slot for mixed of signal counts obeying the BED ( $\mu_{signal}$ ) and dark counts obeying a Poissonian distribution ( $\mu_{dark}$ ). By using Eq. (6), we can calculate  $g^{(2)}(\tau)$ ,  $g^{(3)}(\tau_1, \tau_2)$  and  $g^{(4)}(\tau_1, \tau_2, \tau_3)$  for signal counts mixed with various intensities of dark counts, i.e. under conditions of various SDRs.

We can experimentally confirm this calculation by measuring second-, third- and fourth-order temporal correlations for our pseudo-thermal source for a range of SDRs. During the experiment, the pump power of the up-conversion device is kept at the point where the conversion efficiency is highest, so the dark count rate is fixed. The signal count rate can be adjusted by attenuating photon intensity through a VOA. The SDR is then decreased from 250 to 0.5 in 5dB steps.

Figure 5 shows the zero-delay temporal correlations  $g^{(2)}(0)$ ,  $g^{(3)}(0,0)$  and  $g^{(4)}(0,0,0)$  for both calculated and experimental data, which are in good agreement. When the signal count rate is significantly larger than dark count rate, the peak values of correlations are close to the theoretical values,  $n!$ , for a thermal source; when the signal count rate is reduced and becomes comparable to the dark count rate, the peak values are reduced and approach the expected values for a Poissonian photons. This further demonstrates that dark counts can be treated as a Poissonian distribution in such measurement analysis. From Fig. 5, one can see when the SDR is larger than 100, or 20 dB, the influence of the dark counts on the temporal correlation measurement is negligible. When the signal count rate is lower, a dark count influence becomes obvious. Because the dark counts can be treated as the Poissonian distribution and the SDR can be obtained by directly measuring the signal count rate and dark count rate, the dark count influence on the temporal correlation measurement results can be estimated [34].

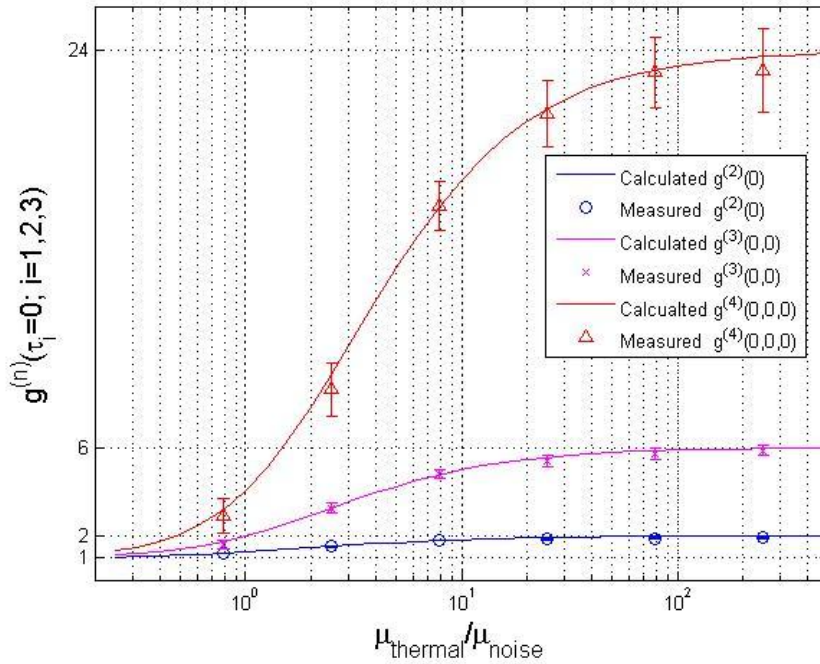


Fig. 5. Calculated and measured  $g^{(2)}(0)$ ,  $g^{(3)}(0,0)$  and  $g^{(4)}(0,0,0)$  values as function of the ratio between signal count rate to dark count rate.

## 5. Conclusion

We demonstrate an approach to measure second-, third- and fourth-order temporal correlations of photons in the NIR region using an up-conversion device. In the experiment, a coherent source and a pseudo-thermal source near 1310 nm are used. We up-convert the NIR photons to the visible region at 710 nm and then perform the temporal correlation measurements using Si-APDs. The experimental results reveal that the temporal correlations of the up-converted photons at 710 nm agree very well with theoretical predictions. In other words, the photon statistics are well preserved in the frequency up-conversion process. In such a measurement, dark counts become an issue when the signal is weak. We further studied the noise from the up-conversion process and its influence on the temporal correlation values. Although the noise photons generated by SRS technically should follow the BED, with their coherence time far too short for our detectors to resolve the thermal bunching, we can treat the dark counts as a Poissonian distribution in our noise analysis for this measurement. We calculated and measured the values of  $g^{(2)}(0)$ ,  $g^{(3)}(0,0)$  and  $g^{(4)}(0,0,0)$  at different SDR levels for a thermal photon source. The measured and calculated results are in good agreement, which provides a way to estimate the dark count influence on the measurement results. In this frequency up-conversion experimental set-up, all components are commercially available and the total single photon detection efficiency is as high as 26%. Therefore, we can conclude that photon statistics are preserved in frequency up-conversion process and this approach is an efficient way to study the temporal correlations of NIR photons.

## Acknowledgments

The authors thank B Baek, NIST, for high order correlation calculation programs. The authors thank OptoElectronic Components and PicoQuant for lending the four-channel time-correlated single photon counting system. This work is supported by the National Institute of Standards and Technology (NIST) quantum information initiative. The identification of any

commercial product or trade name does not imply endorsement or recommendation by the National Institute of Standards and Technology.